– DRAFT – VERSION 0.0.0

Direct Photoproduction of Narrow Strange Baryon Resonance in the Reaction $\gamma p \to p\, K_S K_L$. Reanalysis of the CLAS Data

The CLAS Collaboration
(Dated: October 5, 2021)

This article presents results of yet another analysis based on the same CLAS g11 photoproduction data published elsewere in Refs. [1] and [2]. The search for a purported Θ^+ pentaquark is performed by studying the reaction $\gamma p \to p\, K_S K_L$, where the K_S is reconstructed in the invariant mass of its decay $\pi^+\pi^-$ pairs and the K_L is reconstructed in the missing mass of pK_S. The resonance structure is searched in both, in the missing mass $M_X(K_S)$ as well as in the invariant mass $M(pK_L)$.

Contrary to Ref. [2] and similar to Ref. [1] in this this analysis the events are selected above the ϕ peak. However, instead of "no cut" strategy adopted by Ref. [1] to establish the upper limit of its production, in this paper we made a search by restricting kinematic phase space to avoid possible reflections on the distribution under study from other simultaneously produced competing sub-processes. A clear peak structure is observed in both combinations: in the missing mass of K_S with central value $M_X(K_S) = 1.551 \pm 0.003$ GeV and in the invariant mass of proton and K_S with a central value $M(pK_S) = 1.552 \pm 0.006$ GeV. The Gaussian widths of the observed peaks are found to be $\sigma = 0.019 \pm 0.003$ GeV and $\sigma = 0.024 \pm 0.007$ GeV, respectively, compatible with the experimental resolution. The statistical significance of the observed excess of events, estimated as a log-likelihood ratio of background only and signal+background hypotheses in the missing mass $M_X(K_S)$ is 5.9 σ.

In both combinations of the proton with K_S and K_L, the strangeness is not defined. The observed structure could be either due to previously unknown narrow excited Σ^{*+} resonance or exotic pentaquark state Θ^+ with $uudd\bar{s}$ quark structure.

PACS numbers: 12.38.Aw, 13.60.Rj, 14.20.-c, 25.20.Lj

I. INTRODUCTION

In the early work on Constituent Quark Model (CQM), Gell-Mann already anticipated the existence of multiquark states including tetraquarks and pentaquarks. Our best theory of strong interactions, Quantum Chromodynamics (QCD), does not exclude such quark configurations either [3].

Over the last few years, the LHCb Collaboration reported an observation of four narrow P_c^+ pentaquark states in decays $\Lambda_b^0 \to J/\psi p K^-$, $\Lambda_b^0 \to J/\psi p \pi^-$, and $B_s^0 \to J/\psi p \bar{p}$ with hidden heavy charm quark contributions [4–7].

However, so far, the experimental evidences for the existence of multiquark states with light quark content have never reached the level comparable to that for the LHCb results and conventional hadrons. Although, currently there are lively discussions about the tetraquark mesons, the fate of the pentaquark baryons, especially of those with properties suggested by the chiral quark soliton model [8], has been marred due to the absence of coherent experimental data on their observations. This is partly because of the failure to reproduce previous claims of some experiments in higher statistics measurements, and also due to the large number of reports where pentaquark states were searched for and not observed (in particular, it was not observed by the CLAS analyses of the reaction $\gamma p \to K\overline{K}N$ [1]). A brief experimental overview of the status of the pentaquark searches has been given in Ref. [2], which refers also to the general review papers on pentaquarks.

In Ref. [2], the controversial experimental situation motivated us to exploit interference in a way proposed in Ref. [9] to enhance a possible small signal of a photoproduced baryon resonance (e.g., of a pentaquark) by its interference with the ϕ production amplitude. As a result, the analysis of the reaction $\gamma p \to p\, K_S K_L$, with restriction for $M(K_S K_L)$ to be in the ϕ-peak, led to observation of statistically significant structure in the missing mass of K_S, i.e., in $M(pK_L)$, at the mass of $M(pK_L) = 1.543 \pm 0.002$ GeV. Its interpretation as a new state of matter, however, will gain a very strong support, if the corresponding signal is observed also in a direct production, without invoking the interference. That is why we analyze here the same reaction, based on the same data set, but, instead, with events above the ϕ peak, where a baryon resonance in $pK^0(\overline{K^0})$ system may be produced directly, without the interference enhancement.

Such an analysis was already performed in Ref. [1] and no resonance structure was observed neither in the missing mass of K_S, $M_X(K_S)$ nor in the invariant mass $M(pK_S)$.

In Ref. [1] "no cuts" strategy was adopted. This led to the establishment of the upper limit of the photoproduction cross section of Θ^+. In this paper we significantly improve particle identification of K_S and missing K_L particles. Besides this, to reduce the huge overlap of the competing sub-processes we cut out the phase space of the overlapping reactions.

II. EXPERIMENT

The presented results are based on the same data set collected in 2004 with the CLAS detector [10] at Jefferson Lab and analyzed previously in Refs. [1] and [9]. The experiment was performed using tagged photon beam produced through bremsstrahlung from a 4.02 GeV initial electron beam from the Continuous Electron Beam Accelerator Facility (CEBAF).

In this experiment, the photon beam was incident on a 40 cm long liquid hydrogen target along its axis. The target had 4 cm in diameter and was centered 10 cm upstream from the center of the CLAS detector. The detector consists of six equal sectors, equipped with time-of-flight scintillator counters, Electromagnetic Calorimeters, Drift Chambers and Čerenkov Counters, covering nearly 4π solid angle.

Initial particle identification scheme used to select charged particles in the final state is based on the measurement of momenta and the time of flight of charged particles. The photon beam energy correction and charged particle momentum corrections are based on the code developed for the analysis presented in Ref. [1]. The raw data used in the present analysis were processed in the same way as in Refs. [1] and [2], including corrections for the energy loss of charged particles in the target, uncertainties in the magnetic field, and misalignments of the drift chambers.

III. ANALYSIS

A. Event Selection and Reconstruction of Final State

Events for this analysis are selected requiring at least three charged tracks in the final state identified as a proton, π^+ and π^-. The initial photon is chosen to be within 1 ns of the start time defined by the start counter, and it was required to have only one hit in the tagger within 1.5 ns of the start time.

The K_S is reconstructed in the invariant mass of the π^+ and π^- particles. The second neutral kaon, the K_L, is reconstructed in the missing mass of the three detected particles, $M(K_L)^2 = M_X(pK_S)^2 = (P_\gamma + P_t - P_{K_S} - P_p)^2$, where P_i are four momenta of the photon, target proton, K_S, and final state proton, respectively. The search for a resonance in the KN system can be done either in the invariant mass of the proton and K_S or in the missing mass of K_S, which is the invariant mass of the proton and K_L. However, as can be seen in Fig. 7 of Ref. [1], the final mass distributions for both K_S and K_L still contain significant background contributions.

Therefore, to more clearly identify the reconstructed K_S and the final KN state with a good mass resolution and a better signal to background ratio, we implement the following cuts (hereinafter referred to as vertex cuts) similar to ones used in Ref. [2] and graphically presented in Fig. 1:

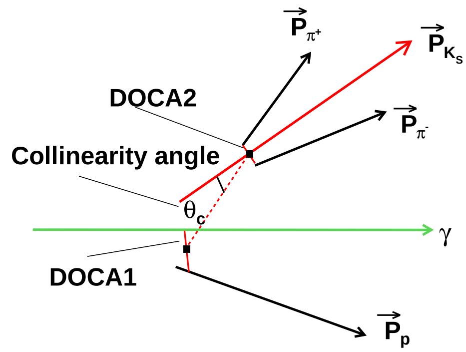

FIG. 1. Reconstruction of K_S decay (see text for explanation).

- The proton track must come with the closest distance not more than 1 cm from the photon beam line (this distance is called hereinafter DOCA1); the midpoint of the shortest line between the proton track and the photon beam line is called the primary vertex.

- The distance of the mutual closest approach of the two pion tracks must be less than 0.75 cm (it is called hereinafter DOCA2); the midpoint of the shortest line between the two pion tracks is called the decay vertex.

- We define the collinearity angle θ_c as the angle between the line connecting the primary and decay vertices and the direction of the three-momentum of the K_S reconstructed as the sum of the two pion momenta. Then we require $\cos\theta_c > 0.97$.

- Decay distance $d > 3$ cm. The decay distance is a distance between the primary and secondary vertices.

In Fig. 2 invariant mass of $\pi^+\pi^-$ pairs for events with $M_X(p\pi^+\pi^-) = 0.496 \pm 0.030$ GeV and $M_X(p) > 1.035$ GeV (to exclude contribution from $\phi(K_S K_L)$ meson) is presented with above mentioned vertex cuts. The data are fitted with Gaussian+Pol(2) function, where Pol(2) is a second order polynomial function. The solid (red) curve is a result of the fit. The dashed (green) curve is resulting Gaussian function from the fit. The background, fitted with Pol(2) function, is presented by dotted (pink) curve. The fit resulted in a mass value $M(\pi^+\pi^-) = 0.499$ GeV with Gaussian width $\sigma = 3.7$ MeV.

In Fig. 3 missing mass $M_X(pK_S)$ for events with $M_X(p) > 1.035$ GeV and $M(\pi^+\pi^-) = 0.499 \pm 0.010$ GeV is presented with the above mentioned vertex cuts. The data are fitted with a Gaussian+Pol(2) function, where Pol(2) is a second order polynomial function. The solid

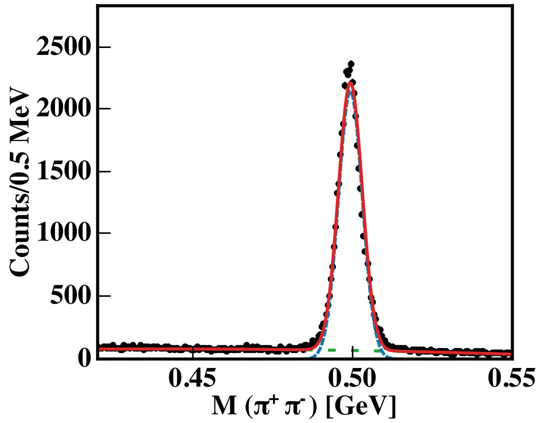

FIG. 2. Invariant mass of $\pi^+\pi^-$ pairs for events with $M_X(p) > 1.035$ GeV and $M_X(p\pi^+\pi^-) = 0.496 \pm 0.030$ GeV. Data are presented with solid points. Solid (red) curve is a result of the fit with Gaussian+Pol(2) function. Dashed (blue) curve is Gaussian function from the fit and the background is presented by dotted (pink) curve.

(red) curve is a result of the fit. The dashed (green) curve is a resulting Gaussian function from the fit. The background, fitted with a Pol(2) function, is presented by dotted (green) curve. The fit resulted in a mass value $M_X(p\pi^+\pi^-) = 0.496$ GeV with a Gaussian width of $\sigma = 9.8$ MeV.

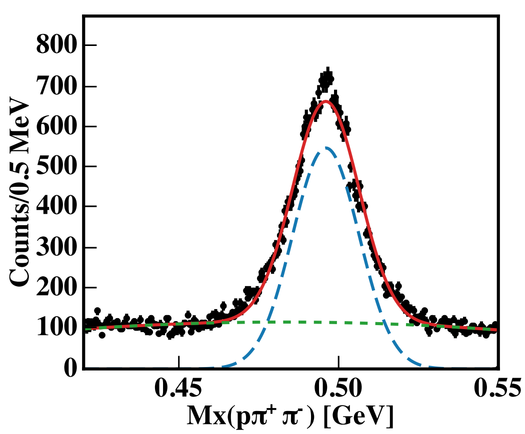

FIG. 3. Missing mass $M_X(pK_S)$ for events with $M_X(p) > 1.035$ GeV and $M(\pi^+\pi^-) = 0.499 \pm 0.010$ GeV. Data are presented with solid points. Solid (red) curve is a result of the fit with Gaussian+Pol(2) function. Dashed (blue) curve is Gaussian function from the fit and the background is presented by dotted (pink) curve.

In Fig. 4, a missing mass of proton, $M_X(p)$, is presented after the following cuts: $M(\pi^+\pi^-) = 0.499 \pm 0.004$ GeV and $M_X(p\pi^+\pi^-) = 0.496 \pm 0.010$ GeV. Data are fitted with a Gaussian+Pol(2) (second order polynomial) function with the results $M(\phi) = 1.022$ GeV and Gaussian width $\sigma = 4.7$ MeV.

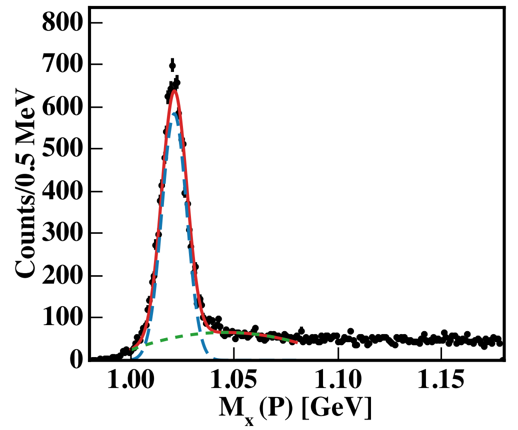

FIG. 4. Missing mass $M_X(p)$ for events with cuts: $M(\pi^+\pi^-) = 0.499 \pm 0.004$ GeV and $M_X(p\pi^+\pi^-) = 0.496 \pm 0.010$ GeV. Data are presented with solid points. Solid (red) curve is a result of the fit with Gaussian+Pol(2) function. Dashed (blue) curve is Gaussian function from the fit and the background is presented by dotted (pink) curve.

In Fig. 5, the invariant mass $M(p\pi^-)$ is presented for events with the following cuts: $M(\pi^+\pi^-) = 0.499 \pm 0.010$ GeV and $M_X(p\pi^+\pi^-) = 0.496 \pm 0.030$ GeV. Data are fitted with a Gaussian+Pol(2) (second order polynomial) function with a results $M(\Lambda) = 1.116$ GeV and Gaussian width $\sigma = 1.7$ MeV. To avoid the reflection from $\Lambda(1116)$, in the following we used a cut $M(p\pi^-) > 1.126$ GeV, as it was done in Ref. [1].

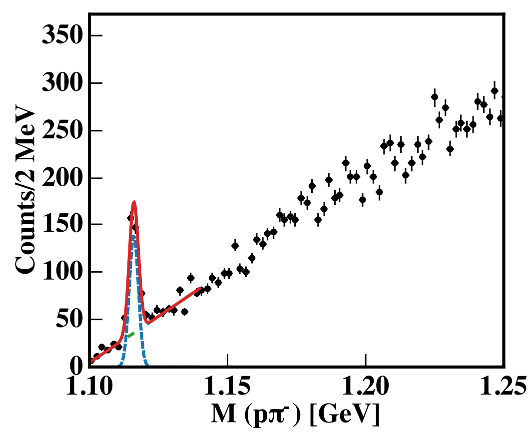

FIG. 5. Invariant mass $M(p\pi^-)$ for events with cuts: $M(\pi^+\pi^-) = 0.499 \pm 0.010$ GeV and $M_X(p\pi^+\pi^-) = 0.496 \pm 0.030$ GeV. Data are presented with solid points. Solid (red) curve is a result of the fit with Gaussian+Pol(2) function. Dashed (green) curve is Gaussian function from the fit and the background is presented by dotted (green) curve.

B. Missing Mass of K_S

Below the search for baryon resonance in pK system is performed in a direct production for the range of the missing mass of proton above the ϕ peak, $M_X(p) > 1.035$ GeV.

Although we have eliminated contribution of the ϕ meson and Λ hyperon, in order to search for a baryon resonance in the missing mass, $M_X(K_S)$, one has to take additional measures to avoid kinematic reflections from excited Σ^* hyperons in $M(pK_S)$ system. Similarly one has to prevent kinematic reflections from excited Σ^*'s in $M_X(K_S)$, when searching for a baryon resonance in $M(pK_S)$ system.

In Fig. 6, we present Dalitz plot $M^2(pK_S)$ vs $M_X^2(K_S)$ for events above the ϕ peak, $M_X(p) > 1.035$ GeV. Other cuts include all above mentioned vertex cuts along with the cuts: $M(\pi^+\pi^-) = 0.499 \pm 0.004$ GeV and $M_X(p\pi^+\pi^-) = 0.496 \pm 0.010$ GeV.

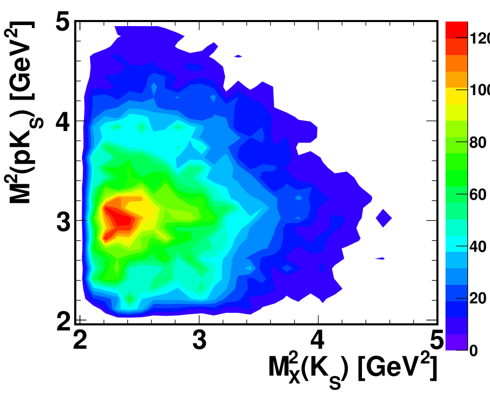

FIG. 6. Dalitz plot $M^2(pK_S)$ versus $M_X^2(K_S)$ for events above the ϕ peak, $M_X(p) > 1.035$ GeV and $M(p\pi^-) > 1.126$ GeV.

In Fig. 7, we present missing mass, $M_X(K_S)$, with different cuts on the invariant mass $M(pK_S)$: a) with no cut on $M(pK_S)$, b) with $M(pK_S) < 1.8$ GeV, c) with $M(pK_S) < 1.7$ GeV, d) with $M(pK_S) < 1.6$ GeV, e) with $M(pK_S) < 1.52$ GeV, and f) with $M(pK_S) < 1.5$ GeV, respectively. As one can see there is a peak structure around 1.55 GeV, which becomes more prominent with decreasing upper limit cuts on $M(pK_S)$.

In Fig. 8, we present missing mass, $M_X(K_S)$, with $M(pK_S) < 1.52$ GeV cut. Experimental data are fitted with a Gaussian+Pol(2) function, where Pol(2) is a second order polynomial. The obtained fit parameters for the peak are $M_X(K_S) = 1.551 \pm 0.003$ GeV and for a Gaussian width $\sigma = 0.019 \pm 0.003$ compatible with experimental resolution. Statistical significance of the observed peak estimated as log-likelihood ratio, calculated as in [9], is $\sim 5.3\sigma$. A phase space Monte Carlo (MC) generator used with the full chain of the CLAS simulation and reconstruction program is normalized in

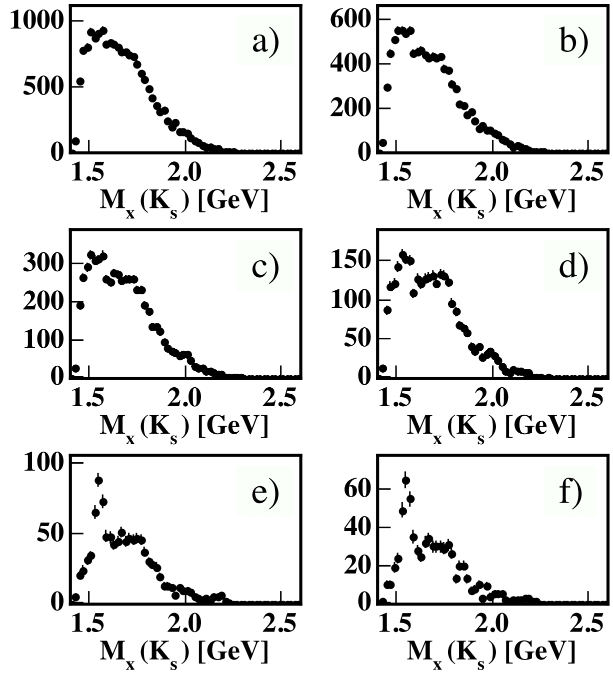

FIG. 7. Count per 20 MeV bin vs missing mass, $M_X(K_S)$: a) no cut on $M(pK_S)$, b), c), d), e), and f) with the upper cut on $M(pK_S)$ 1.80, 1.70, 1.60, 1.52, and 1.5 GeV, respectively.

the region below 1.5 GeV and above 1.9 GeV ouside of possible Σ^* resonances. The corresponding MC simulated solid (green) histogram with all our cuts applied is a smooth function without any peak structure. Excess of events above 1.6 GeV in data can be attributed to the well known heavy excited Σ^* recorded in Ref. [11]. However, the narrow peak at $\sim$1.55 GeV is previously unobserved structure, which could be due to either another unobserved Σ^* state, or purported Θ^+ pentaquark.

To check the stability of the observed signal, we divided data into two chronologically separated distinct run periods with similar statistics. In Fig. 9, we present $M_X(K_S)$ for both parts. Statistical significance in the first part is estimated as log-likelihood is found to be 3.3σ while in the second part it is 3.3σ.

In the Ref. [2], it was hypothesized a strong $|t_\Theta|$ dependence of the observed structure. Below in Fig. 10, we present missing mass, $M_X(K_S)$, distribution with a different cuts on $|t_\Theta|$.

As we observe, with the stricter cuts the background under the peak drops faster than the signal itself, indicating that the signal is more concentrated at small $|t_\Theta|$, than the background.

The possibility to make the CLAS acceptance more favorable at lower $|t_\Theta|$ values is provided by selecting higher separation of primary and decay vertices. Indeed, larger decay distances correspond to the higher laboratory three momenta of K_S, which would lead to the lower $|t_\Theta|$ and favor production of Θ^+ if its production has

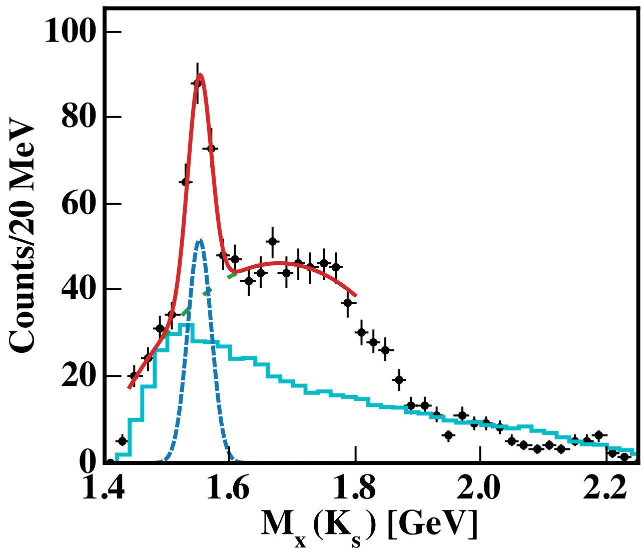

FIG. 8. Missing mass, $M_X(K_S)$ with a cut $M(pK_S) < 1.52$ GeV, same as Fig. 7e. Mean value is 1.551 ± 0.003 GeV and $\sigma = 0.019\pm$ 0.003 GeV. For range $\pm 2\sigma$: signal yield is 120 and background $B = 142$. The log likelihood method gives a significance of 5.3σ. Filled squares are data points. Solid (red) curve is a result of the fit with a Gaussian+Pol(2) function. Dashed (blue) curve is Gaussian function obtained from the fit and the background is presented by dotted (pink) curve. The solid histogram (cyan) is obtained by phase space Monte Carlo simulation.

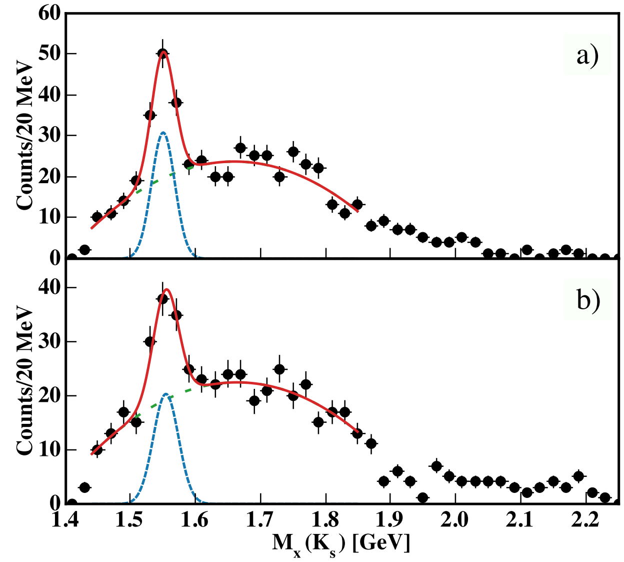

FIG. 9. Missing mass, $M_X(K_S)$ with a cut $M(pK_S) < 1.52$ GeV. a) is for the first part of g11a data, and the lower panel, b) is for the second part of g11a. Filled squares are data. Solid (red) curve is a result of the fit with Gaussian+Pol(2) function. In both panels dotted (cyan) histogram is Gaussian function from the fit and the background is presented by dashed (cyan) curve. The mean value of the upper histogram is 1.550 ± 0.004 GeV, Gaussian $\sigma = 0.018$ GeV. The number of signal events is 65, the number of background events is 69. In the second part, lower panel b) the mean value is 1.554 ± 0.006, the Gaussian $\sigma = 0.019 \pm 0.005$ GeV. Significances calculated from the log-likelihood ratios in the upper panel is 3.3σ on the lower one is 3.1σ

steeper $|t_{\gamma K_S}|$-dependence compared to that of other processes composing the main background. In Fig. 11, we present the ratio of number of events with decay distance $d > 10$ cm over number of events with $d > 3$ cm for the range of $M_X(K_S) < 1.6$ GeV and $M(pK_S) < 1.54$ GeV. All other vertex cuts are the same as before in both cases. As one can see by selecting events with $d > 10$ cm the higher values of $|t_{\gamma K_S}|$ are less preferable, which should suppress higher masses in the missing mass $M_X(K_S)$ more than the peak at ~ 1.55 GeV, due to its steeper $|t_{\gamma K_S}|$-dependence.

In Fig. 12, we present distribution of $M_X(K_S)$ with a cut on K_S decay distance $d > 10$ cm as compared to $d > 3$ cm used in the previous $M_X(K_S)$ distributions. As one can see the region of higher masses is suppressed much more than the peak itself. Although the statistical significance of the peak doesn't change much $\sim 5.9\sigma$, the fact that entire distribution outside of the peak drops very significantly gives further confidence that the observed peak is real.

C. Invariant Mass $M(pK_S)$

Next in Fig. 13, we try to search for the resonance in the invariant mass $M(pK_S)$ with a cut $M(pK_L) < 1.5$ GeV. Although this channel and the missing mass, $M_X(K_S)$, have very different acceptances, the signal is observed with log-likelihood significance of $\sim 3.1\sigma$ at invariant mass $M(pK_S) \sim 1.55$ GeV. The vertex cuts applied include $DOCA1 < 1.0$ cm, $DOCA2 < 0.7$ cm, $\cos\Theta_c > 0.95$ and K_S decay distance $d > 3$ cm.

In Fig. 14 left panel, we present distribution of events in the invariant mass $M(pK_S)$ together with $M(pK_L)$ distribution. As this two channels have very different acceptances the shape of the distributions look very different. For the sake of uniformity we keep all cuts similar. These include upper limit Dalitz plot cuts on the opposite $M(pK)$ system to be below 1.5 GeV with the following common vertex cuts: $DOCA1 < 1.0$ cm, $DOCA2 < 0.7$ cm, $\cos\Theta_c > 0.95$ and K_S decay distance $d > 3$ cm.

After the acceptance correction Fig. 14 right panel these two distributions have very similar shape. As one can see from the Fig. 15 the acceptance function, i.e., the ratio of MC events accepted by the CLAS over generated one, presented in Fig. 15, indeed is very different for these two channels. However consistent appearance of

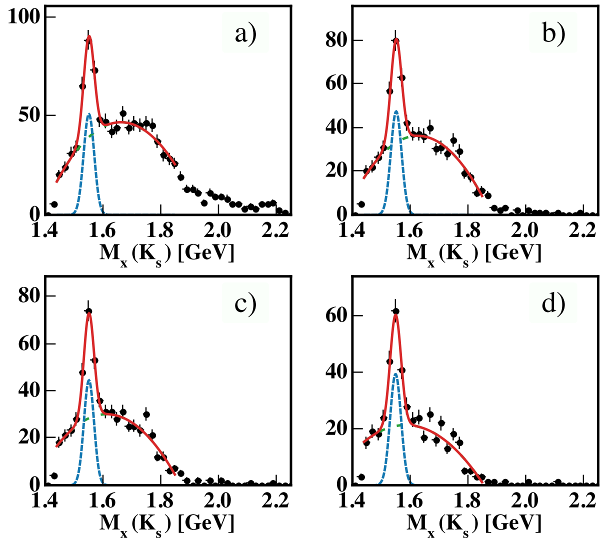

FIG. 10. Missing mass, $M_X(K_S)$ (counts per 20 MeV bin) for $M(pK_S) < 1.52$ GeV with the following cuts: a) no cut on $|t_\Theta|$, b) $|t_\Theta| < 0.85$ GeV^2, c) $|t_\Theta| < 0.75$ GeV^2, d) $|t_\Theta| < 0.65$ GeV^2. Solid (red) curve is a result of the fit with Gaussian+Pol(2) function.

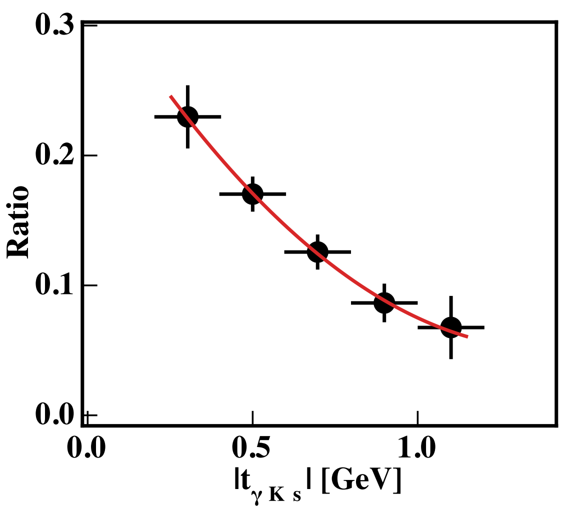

FIG. 11. Ratio of number of events with decay distance $d > 10$ cm over number of events with $d > 3$ cm versus four-momentum transfer $|t_{\gamma K_S}|$ for the range of $M_X(K_S) < 1.6$ GeV and $M(pK_S) < 1.54$ GeV.

the structure around 1.55 GeV in both channels provides further confidence that the observed structure is not an artifact of the reconstruction and analysis procedure, or malfunctioning of the CLAS experimental setup.

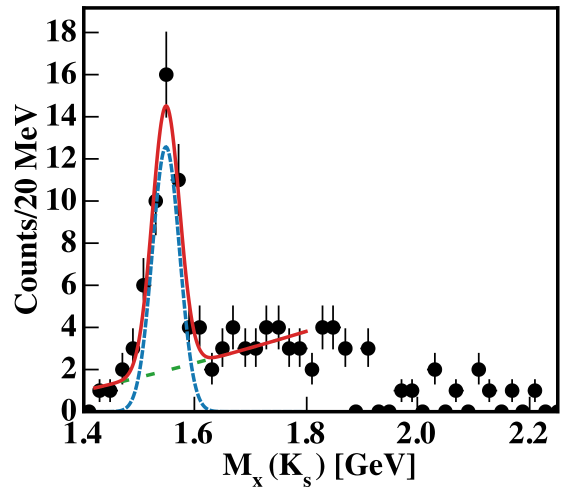

FIG. 12. Missing mass, $M_X(K_S)$ with a cut $M(pK_S) <$ 1.52 GeV, but with decay distance $d > 10$ cm. Mean value is 1.5501 ± 0.0054 GeV and $\sigma = 0.0246 \pm 0.0060$ GeV. For the range of $\pm 2\sigma$: yield is 37 and background $B = 12$. Then the log likelihood method gives a significance of $= 5.9\sigma$. Filled squares are data points. Solid (red) curve is a result of the fit with Gaussian+Pol(2) function. Short dashed (blue) curve is Gaussian function obtained from the fit and the background is presented by the long dashed (green) curve.

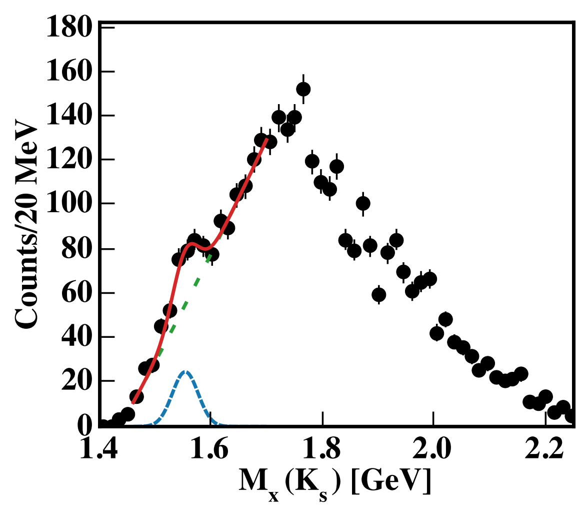

FIG. 13. Invariant mass, $M(pK_S)$ with a cut $M_X(K_S) <$ 1.5 GeV. Solid (red) curve is a result of the fit with Gaussian+Pol(2) function. The short dashed (green) curve is a Gaussian function obtained from the fit and the background is presented by the long dashed (blue) curve. The mean value of the peak is 1.550 ± 0.006 GeV, the Gaussian width is 0.024 GeV. The significance estimated as log-likelihood is 3.1σ.

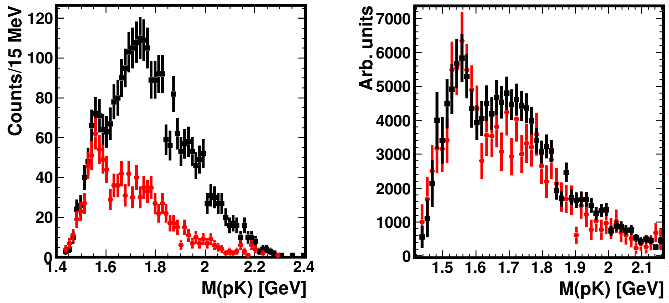

FIG. 14. Left panel: invariant mass $M(pK_S)$ with a cut $M_X(K_S) < 1.5$ GeV squared (black) points (same histogram as in Fig. 13) and missing mass $M_X(K_S) = M(pK_L)$ with a cut $M(pK_S) < 1.5$ GeV circled (red) points. All other cuts are the same: $DOCA1 < 1.0$ cm, $DOCA2 < 0.7$ cm, $\cos\Theta_c > 0.95$ and K_S decay distance $d > 3$ cm. Right panel: the same histograms after acceptance correction.

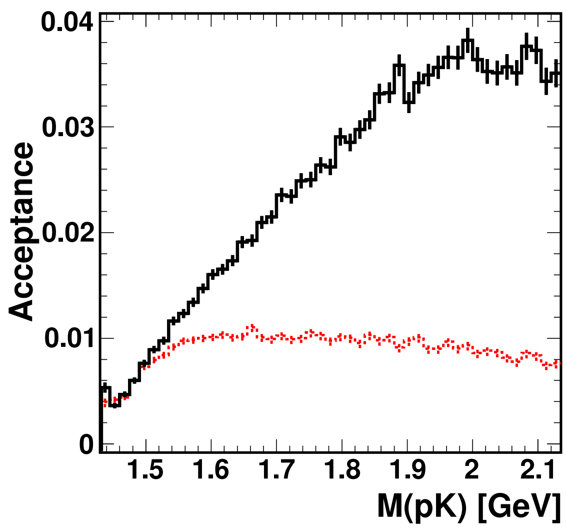

FIG. 15. The acceptance function for $M(pK_S)$ distribution, solid (black) histogram, and $M(pK_L)$ distribution, dashed (red) histogram.

IV. SUMMARY

In summary, in this paper, we present results of reanalysis of the CLAS photoproduction data obtained in the reaction $\gamma p \to p\pi^+\pi^- X$. The K_S is reconstructed in the invariant mass of $\pi^+\pi^-$. The missing particle is identified as another neutral kaon, the K_L, by the missing mass in respect to the proton and K_S. In this analysis the overall particle reconstruction technique led to the better signal to background ratio of reconstructed particles. In addition, as in this reaction after particle reconstruction we have three body final state, ee treat it using Dalitz plot by cutting out not only the ϕ meson in $K_S K_L$ system, but also restricting the invariant mass $M(pK_S)$, when searching for the peak in the missing mass of K_S, $M(pK_L)$, and vice versa, to suppress kinematical reflections from the opposite pK system. The observed peak at $\sim$1.55 GeV in the missing mass $M(K_S)$ has statistical significance $\sim 5.9\sigma$. It has to be mentioned that here, for the first time in the pentaquark searches, we performed sampling of collected data into two statistically equal run periods and observed a peak in the missing mass distribution, $M_X(K_S)$, in both of them. At the same time and due to very different CLAS acceptances for the invariant mass $M(pK_S)$ compared to the missing $M_X(K_S)$, we observed less prominent peak in the invariant mass $M(pK_S)$. All observed peaks have consistent properties, their positions and widths agree with each other within experimental uncertainties.

Thus, although it is not possible to fix the strangeness of the neutral kaons, presented refined analysis of the same CLAS data demonstrates first of all that there is a new narrow peak, and secondly, that the possibility of the observed peak being due to the Θ^+ pentaquark, is favorable. The latter possibility would be excluded only, if the observed peaks were due to yet unobserved narrow excited Σ^* resonance. However the fact that no Σ^* resonance is observed in $\Lambda\pi$ or $\Sigma\pi$ channels, makes unlikely for the peak to be due to the excited Σ^* resonance.

The strangeness conservation in all photoproduction experiments for the search of the Θ^+ leads to the multiparticle final states. Therefore the reflections from different combinations are unavoidable. The crucial experiment to rule out such a complicated overlap of different sub-processes could be done in experiments with a kaon beams to produce purported Θ^+ pentaquark in the formation reactions such as $K^+n \to \Theta^+ \to K^0 p$ or $K_L + p \to \Theta^+ \to K^+ n$. The proposed experiment with the K-long beam in Hall D [12] is well suited for this purpose, as was discussed also in Ref. [13].

V. ACKNOWLEDGMENTS

We would like to acknowledge the outstanding efforts of the staff of the Accelerator and the Physics Divisions at Jefferson Lab that made the experiment possible. This work was supported in part by the Italian Istituto Nazionale di Fisica Nucleare, the French Centre National de la Recherche Scientifique and Commissariat a l'Energie Atomique, the US Department of Energy and National Science Foundation, and the Korea Science and Engineering Foundation. The Southeastern Universities Research Association (SURA) operates the Thomas Jafferson National Accelerator Facility for the United States Department of Energy under contract No. DEAC05-84ER40150.

[1] R. De Vita *et al.* [CLAS Collaboration], "Search for the Θ^+ pentaquark in the reactions $\gamma p \to \overline{K^0}K^+n$ and $\gamma p \to \overline{K^0}K^0p$," Phys. Rev. D **74**, 032001 (2006).

[2] M. J. Amaryan, G. Gavalian, C. Nepali, M. V. Polyakov, Y. Azimov, W. J. Briscoe, G. E. Dodge, C. E. Hyde, F. Klein, V. Kuznetsov, I. Strakovsky, and J. Zhang, "Observation of a narrow structure in $p(\gamma, K_S)X$ via interference with ϕ-meson production," Phys. Rev. C **85**, 035209 (2012).

[3] M. Gell-Mann, "A schematic model of baryons and mesons," Phys. Lett. **8**, 214 (1964).

[4] R. Aaij *et al.* [LHCb Collaboration], "Observation of $J/\psi p$ resonances consistent with pentaquark states in $\Lambda_b^0 \to J/\psi K^- p$ decays," Phys. Rev. Lett. **115**, 072001 (2015).

[5] R. Aaij *et al.* [LHCb Collaboration], "Evidence for exotic hadron contributions to $\Lambda_b^0 \to J/\psi p \pi^-$ decays," Phys. Rev. Lett. **117**, 082003 (2016).

[6] R. Aaij *et al.* [LHCb Collaboration], "Observation of a narrow pentaquark state, $P_c(4312)^+$, and of two-peak structure of the $P_c(4450)^+$," Phys. Rev. Lett. **122**, 222001 (2019).

[7] R. Aaij *et al.* [LHCb Collaboration], "Evidence for a new structure in the $J/\psi p$ and $J/\psi \bar{p}$ systems in $B_s^0 \to J/\psi p \bar{p}$ decays," [arXiv:2108.04720 [hep-ex]].

[8] D. Diakonov, V. Petrov, and M. V. Polyakov, "Exotic anti-decuplet of baryons: Prediction from chiral solitons," Z. Phys. A **359**, 305 (1997).

[9] M. Amarian, D. Diakonov, and M. V. Polyakov, "To see the exotic Θ^+ baryon from interference," Phys. Rev. D **78**, 074003 (2008).

[10] B. A. Mecking *et al.* [CLAS Collaboration], "The CEBAF Large Acceptance Spectrometer (CLAS)," Nucl. Instrum. Meth. A **503**, 513 (2003).

[11] P. A. Zyla *et al.* [Particle Data Group], "Review of Particle Physics," PTEP **2020**, 083C01 (2020).

[12] "Strange hadron spectroscopy with secondary KL beam in Hall D," Spokespersons: M. Amaryan, M. Bashkanov, S. Dobbs, J. Ritman, J. Stevens, and I. Strakovsky, [KLF Collaboration], JLab Proposal C12–19–001, Newport News, VA, USA, 2020. [arXiv:2008.08215 [nucl-ex]].

[13] A. Thiel and E. Klempt, "Highlights of the spectroscopy of hyperons and cascade baryons," [arXiv:2005.06971 [nucl-ex]].